Photofunctional Vesicles Containing Prussian Blue and Azobenzene

Y. Einaga,[†,||] O. Sato,[‡] T. Iyoda,[§] A. Fujishima,*[,†,‡] and K. Hashimoto*[,‡,⊥]

Contribution from the Department of Applied Chemistry, The University of Tokyo, 7-3-1 Hongo, Bunkyo-ku, Tokyo 113-8656, Japan, Kanagawa Academy of Science and Technology, Atsugi, Kanagawa 243-0297, Japan, Department of Applied Chemistry, Tokyo Metropolitan University, 1-1 Minami-Osawa, Hachioji, Tokyo 192-0397, Japan, and Research Center for Advanced Science and Technology, The University of Tokyo, 4-6-1 Komaba, Meguro-ku, Tokyo 153-8904, Japan

Received July 13, 1998

Abstract: The intercalation of inorganic materials into organized organic assemblies presents many opportunities for the development of new functional materials with superior physicochemical properties. We have designed a composite material comprising Prussian blue intercalated into photoresponsive organic molecules (azobenzene-containing multibilayer vesicles). Photoisomerization in the solid system was achieved by diluting the azobenzene-containing bilayer membrane in a poly(vinyl alcohol) matrix. The photoisomerization of the film was accompanied by a geometrically confined structural change within the vesicles, as reflected by changes in the dipole moment and electrostatic field. As a result, we were able to control the magnetic properties of this material by photoillumination.

Introduction

Research into artificial membrane-forming lipids such as liposomes has attracted much attention in recent years.[1] Liposomes (vesicles) are spherically closed lipid bilayers which, by analogy to the cell membrane, enclose an aqueous compartment and are suitable for a wide variety of biophysical and biochemical investigations.[2−5]It has been reported that cast films of synthetic bilayer membranes provide ordered molecular architectures at the molecular level as well as at the macroscopic level.[6−8] Furthermore, the use of organized organic assemblies to direct the formation of mesoscopic inorganic structures under mild conditions is of topical interest.[1,9−11] In particular, attempts to intercalate inorganic materials into functional organic molecules offer many possibilities for developing novel functional materials whose physicochemical properties are superior to those of conventional materials.

Likewise, the design and synthesis of functional materials with nanometer dimensions (mesoscopic materials) are also subjects of intense current research. Although several studies have been devoted to the synthesis of nanometer-sized compound semiconductors, relatively little work exists for magnetic materials of similar dimensions.[12−15] On the other hand, the design of molecule-based materials has been attracting increasing attention in the field of magnetism.[16−18] One of the current topics of interest in this field is the reversible control of physical properties in solid-state compounds with magnetic properties that can be controlled by external stimuli, such as photoillumination.[19,20] We have focused our attention on the combination of photoisomerizable vesicles and a molecule-based magnet in order to produce a new photofunctional system.

For the work reported herein, we have designed composite materials, comprising Prussian blue (a ferromagnet at low temperature) and photoresponsive organic molecules (azobenzene-containing multibilayer vesicles), whose magnetic properties can be controlled by photoillumination. Normally, photoisomerization of azobenzene-containing materials does not occur in the solid state because photoisomerization is accompanied by a large volume change.[21] We have succeeded not only in intercalating Prussian blue into an organic solid system but also in making the cis−trans photoisomerization possible at low temperatures in the solid system by diluting the azobenzene-

* To whom correspondence should be addressed.
† Department of Applied Chemistry, The University of Tokyo.
‡ Kanagawa Academy of Science and Technology.
§ Tokyo Metropolitan University.
⊥ Research Center for Advanced Science and Technology, The University of Tokyo.
|| Research Fellow of the Japan Society for the Promotion of Science.

(1) Fendler, J. H. *Chem. Rev.* **1987**, *87*, 877.
(2) Walker, S. A.; Kennedy, M. T.; Zasadzinski, J. A. *Nature* **1997**, *387*, 61.
(3) Bangham, A. D. *Chem. Phys. Lipids* **1993**, *64*, 275.
(4) Yogev, D.; Guillaume, B. C. R.; Fendler, J. H. *Langmuir* **1991**, *7*, 623.
(5) Bangham, A. D.; Standish, M. M.; Watkins J. C. *J. Mol. Biol.* **1965**, *13*, 238.
(6) Ishikawa, Y.; Kunitake, T. *J. Am. Chem. Soc.* **1991**, *113*, 621.
(7) Kunitake, T.; Kimizuka, N.; Higashi, N.; Nakashima, N. *J. Am. Chem. Soc.* **1984**, *106*, 1978.
(8) Shimomura, M.; Ando, R.; Kunitake, T. *Ber. Bunsen-Ges. Phys. Chem.* **1983**, *87*, 1134.
(9) Mann, S.; Archibald, D. D.; Didymus, J. M.; Douglas, T.; Heywood, B. R.; Meldrum, F. C.; Reeves, N. J. *Science* **1993**, *261*, 1286.
(10) Ozin, G. A. *Adv. Mater.* **1992**, *4*, 612.
(11) Kanatzidis, M. C.; Wu, C.-G.; Marey, H. O.; Kannewurf, C. R. *J. Am. Chem. Soc.* **1989**, *111*, 4139.
(12) Ziolo, R. F.; Giannelis, E. P.; Weinstein, B. A.; O'Horo, M. P.; Ganguly, B. N.; Mehrotra, V.; Russell, M. W.; Huffman, D. R. *Science* **1992**, *257*, 219.
(13) Okada, H.; Sakata, K.; Kunitake, T. *Chem. Mater.* **1990**, *2*, 89.
(14) Papaefthymiou, V.; Kostikas, A.; Simopoulos, A.; Niarchos, D.; Gangopadyay, S.; Hadjipanayis, G. C.; Sorensen, C. M.; Klabunde, K. J. *J. Appl. Phys.* **1990**, *67*, 4487.
(15) Zhao, X. K.; Herve, P. J.; Fendler, J. H. *J. Phys. Chem.* **1989**, *93*, 908.
(16) Kahn, O. *Molecular Magnetism*; VCH: New York, 1993.
(17) Ferlay, S.; Mallah, T.; Ouahes, R.; Veillet, P.; Verdaguer, M. *Nature* **1995**, *378*, 701.
(18) Entley, W. R.; Girolami, G. S. *Science* **1995**, *268*, 397.
(19) Sato, O.; Einaga, Y.; Iyoda, T.; Fujishima, A.; Hashimoto, K. *J. Electrochem. Soc.* **1997**, *144*, L11.
(20) Sato, O.; Iyoda, T.; Fujishima, A.; Hashimoto, K. *Science* **1996**, *272*, 704.
(21) Nakahara, H.; Fukuda, K.; Shimomura, M.; Kunitake, T. *Nippon Kagaku Kaishi* **1988**, *7*, 1001.

10.1021/ja982450l CCC: $18.00
Published on Web 04/02/1999

containing bilayer membrane in a poly(vinyl alcohol) matrix. The observed changes in dipole moment and electrostatic field suggest that photoisomerization is accompanied by a geometrically confined structural change. Thus, the magnetization values of the vesicles at low temperature could be switched reversibly by UV and visible light illumination.

Experimental Section

Preparation of Composite Film. Compound **1**, a commercially available double-chain ammonium amphiphile, didodecyl dimethylammonium bromide (**1** = $[CH_3(CH_2)_{11}]_2(CH_3)_2N^+Br^-$), was obtained from Aldrich. An azobenzene-containing amphiphile **2** (=$C_{12}AzoC_5N^+Br^-$) was synthesized according to a procedure reported previously.[8]

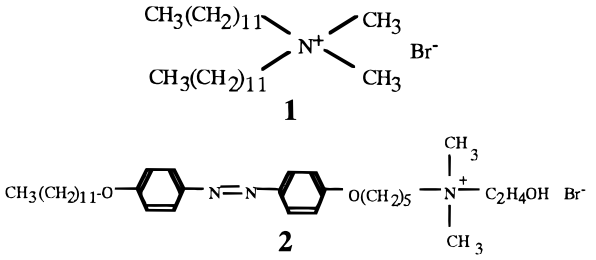

The photoisomerizable composite film was prepared as follows. A sonicated clear solution containing amphiphiles **1** (10 mM) and **2** (10 mM) was prepared in deionized H_2O, and the dispersion was mixed with an aqueous solution of poly(vinyl alcohol) (PVA, MW ≈ 70 000; PVA, 200 mg; H_2O, 4 mL). PVA acts as a matrix for **2** (mixing weight ratio, **1**:**2**:PVA = 10:1:170). Other investigators have reported that composite thin films composed of an amphiphile-based bilayer membrane and PVA form well-ordered bilayer structures.[22,23] The composite film, hereafter designated film **3** (=**1** + **2** + PVA), was prepared by casting the above solution on a clean glass plate (pretreated with concentrated sulfuric acid) at room temperature.

Intercalation. The molecule-based magnetic compound was intercalated into the bilayer membranes following a stepwise ion-exchange procedure.[24] This methodology is schematically depicted in Figure 1. A film containing **1** only was prepared by casting an aqueous solution of **1** (10 mM) on a clean glass plate at room temperature; the cast film was then thoroughly dried in vacuo. Bilayer vesicles (Figure 1a) formed in the cast film. Intercalation of the magnetic material was carried out as follows. The cast film containing **1** was first dipped in aqueous $K_3Fe^{III}(CN)_6$ solution (100 mM, for 1 day at room temperature) to exchange the ferricyanide anion with the bromide ion. After being washed with deionized H_2O, the compound (designated **1**-Fe$(CN)_6$) (Figure 1b) was dipped in aqueous $Fe^{II}Cl_2$ solution (100 mM, for 1 day at room temperature). After being washed, it was kept in deionized water for 1 h to remove unreacted Fe^{2+} ion (compound designated **1**-Fe$(CN)_6$-Fe) (Figure 1c).

When we intercalated Prussian blue into the composite cast film **3**, a similar method was also applied. A sample of cast film **3** was immersed in an aqueous solution of $K_3Fe^{III}(CN)_6$ (100 mM) for 1 day at room temperature to enable anion exchange with the bromide ion. After being washed with deionized H_2O, the sample goes into suspension as an aqueous gel, which was recast on a clean glass plate (designated film **3**-Fe$(CN)_6$). To prepare the Fe−CN−Fe framework, the **3**-Fe$(CN)_6$ film was next immersed in an aqueous solution of $Fe^{II}Cl_2$ (100 mM) for 1 day at room temperature. After being washed thoroughly with deionized H_2O, it was kept in H_2O for 1 h to remove unreacted Fe^{2+} ion (designated film **3**-Fe$(CN)_6$-Fe).

Physical Methods. An ultrasonicator (Bioruptor, Cosmo Bio, model UCD-200TM) was used (200 W, 30 min) to prepare a clear solution containing vesicles. A scanning electron microscope (SEM, model JMS-6100, JEOL) was used for imaging the vesicles, and the local chemical compositions of the samples were obtained using an energy-dispersive X-ray spectrometer (EDS, model JED-2100). To enhance their visibility, the vesicles were stained with a 0.5% aqueous solution of RuO_4. ^{57}Fe Mössbauer spectra were measured at room temperature using a Wissel MVT-1000 type spectrometer with a $^{57}Co/Rh$ source in the transmission mode. Magnetic properties were investigated with a superconducting quantum interference device (SQUID) magnetometer (model MPMS-5S, Quantum Design). UV−visible absorption spectra were recorded on a UV-3100 spectrophotometer (Shimadzu). The UV−vis measurements at low temperature were performed with a closed-cycle helium refrigerator (Iwatani. Co., Ltd.). UV illumination (filtered light, λ_{max} = 360 nm, 1.0 mW/cm^2) was carried out using an ultrahigh-pressure mercury lamp (HYPERCURE 200, Yamashita Denso). Similarly, visible light illumination (400−700 nm, 1.0 mW/cm^2) was carried out using a xenon lamp (XFL-300, Yamashita Denso).

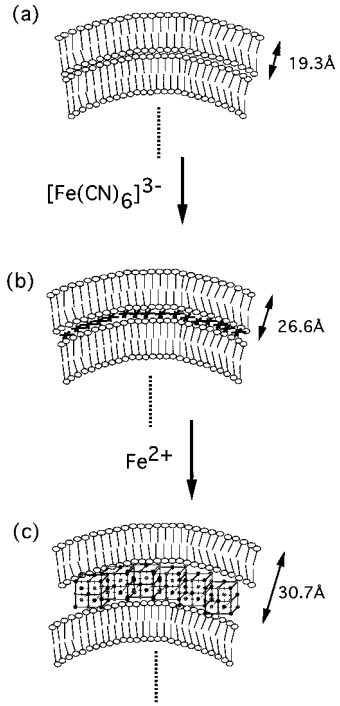

Figure 1. Schematic illustration of the stepwise synthesis of the molecule-based magnet, Prussian blue in vesicles. Cast films of (a) **1**, (b) **1**-Fe$(CN)_6$, and (c) **1**-Fe$(CN)_6$-Fe exhibited a series of X-ray diffraction patterns that correspond to the long-distance spacings, 19.3, 26.6, and 30.7 Å, respectively, up to the fifth order. It is clear that the ordered bilayer structure remains intact during complex formation. In addition, the **1**-Fe$(CN)_6$-Fe film exhibited another diffraction peak at $2\theta = 17.5°$ (5.1 Å), which is ascribed to the Fe^{II}−CN−Fe^{III} framework in the cast film.

Results and Discussion

Photoisomerizable Composite Films. The absorption spectra for the (**2** + PVA) film (dotted curve) and the film **3** (=**1** + **2** + PVA) (solid curve) are shown in Figure 2a. The difference between these spectra is explained by the dilution of **2** (containing azobenzene) with **1** (dialkylammonium matrix), as shown schematically in Figure 2b.[25] A similar dilution process was reported in which differential scanning calorimetry was used to confirm the reaction.[26,27] A scanning electron micrograph (SEM) image of film **3** indicates the presence of ringlike and spheroidal objects of heterogeneous diameters (diameter 1000−

(22) Kunitake, T.; Higashi, N.; Kajiyama, T. *Chem. Lett.* **1984**, 717.
(23) Takahara, A.; Higashi, N.; Kunitake, T.; Kajiyama, T. *Macromolecules* **1988**, *21*, 2443.
(24) Kimizuka, N.; Handa, T.; Kunitake, T. *Mol. Cryst. Liq. Cryst.* **1996**, *277*, 189.
(25) Shimomura, M.; Kunitake, T. *Chem. Lett.* **1981**, 1001.
(26) Okahata, Y.; Ando, R.; Kunitake, T. *Ber. Bunsen-Ges. Phys. Chem.* **1981**, *85*, 789.
(27) Kunitake, T.; Nakashima, N.; Shimomura, M.; Okahata, Y.; Kano, K.; Ogawa, T. *J. Am. Chem. Soc.* **1980**, *102*, 6642.

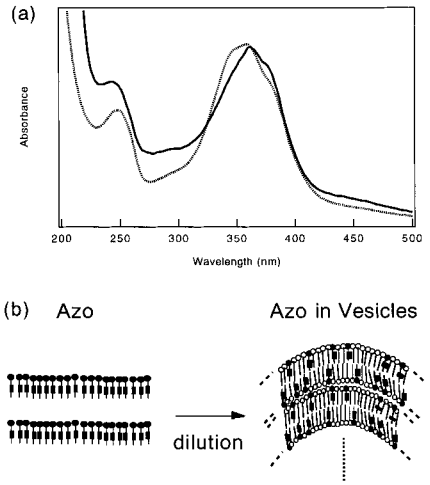

Figure 2. (a) Optical absorption spectra of the (**2** + PVA) film, containing stacked azobenzene moieties (- - -) and film **3** (=**1** + **2** + PVA), containing isolated azobenzene moieties (—). (b) Schematic illustrations of the (**2** + PVA) film and film **3**.

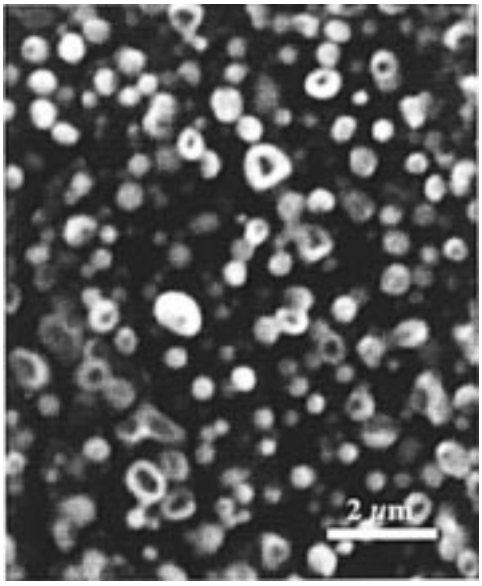

Figure 3. SEM image of **3** (=**1** + **2** + PVA). A 0.5% aqueous solution of RuO_4 was used to stain the vesicles and improve their visibility.

5000 Å) (Figure 3). This image is similar to that for vesicles formed from **1** observed in a cast film without PVA.[28]

Photoisomerization of film **3** was monitored by UV−vis absorption spectroscopy. The typical UV−vis spectral changes due to the photoisomerization are shown in Figure 4. Before illumination, the film consisted of only the trans form of the azo compound because it is thermodynamically more stable than the cis form.[29] At room temperature (Figure 4a), UV illumination of the trans isomer converted it to the cis isomer (process (i) in Figure 4a). The peak at around 360 nm decreased, while new peaks appeared at 450 and 320 nm. The 450- and 320-nm peaks are ascribed to the n−π* and π−π* transitions of the cis isomer, respectively.[30] After subsequent illumination with visible light, the reverse process, i.e., the cis-to-trans isomerization, proceeded completely (process (ii) in Figure 4a). Therefore, the spectra obtained before and after the complete UV illumination−visible illumination cycle were identical. At 12 K, however, very little

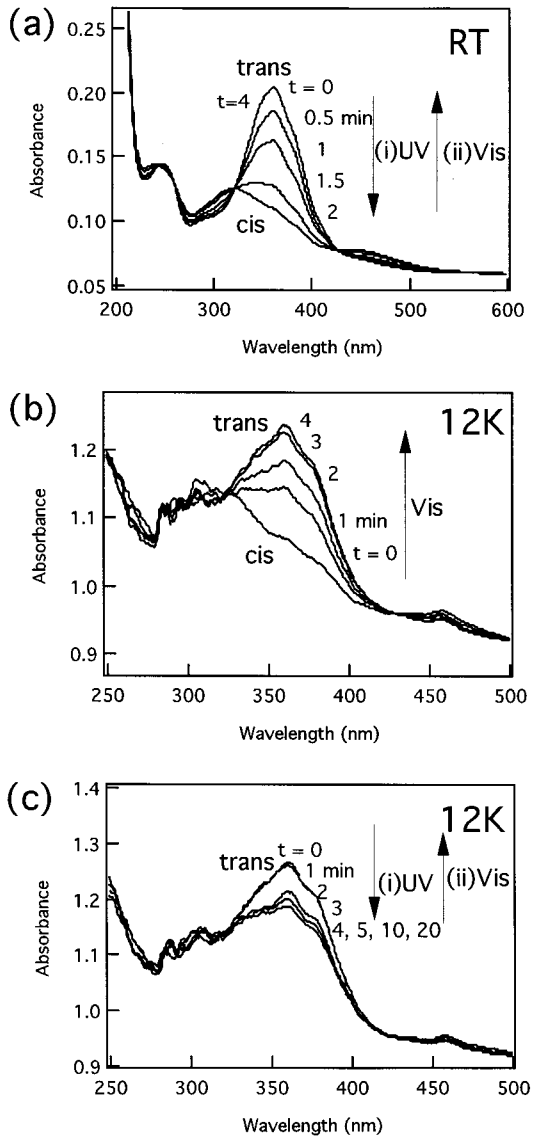

Figure 4. Changes in the optical absorption spectra for film **3** due to photoisomerization. (a) At room temperature, the initial trans state was first illuminated with UV light (360 nm, 1.0 mW/cm^2) for 2 min. Spectra were recorded every 0.5 min during the illumination. Then the isomerized cis state was illuminated with visible light (400−700 nm, 1.0 mW/cm^2) for 2 min. The spectrum at time t = 4 min (after 2 min of UV illumination followed by 2 min of visible light illumination) was identical to that at time t = 0 (before illumination). (b) At 12 K, the initial cis state was prepared by illuminating the trans film at room temperature, followed by cooling the film to 12 K. Then the cis film was illuminated with visible light for 4 min. The spectra were recorded every 1 min during the illumination. (c) Also at 12 K, further illumination, with UV light, of the trans film obtained by the process described in (b). The spectra were recorded every 1 min, and the change saturated after 4 min illumination, at ca. 60% cis. Subsequently, trans−cis photoisomerization cycles were repeated by alternate illumination with UV and visible light.

trans-to-cis photoisomerization was observed, even after UV illumination for much longer times (figure not shown). This is because the photoisomerization of azobenzene derivatives, particularly the trans-to-cis isomerization reaction, is accompanied by an increase in molecular volume. In fact, it is known that the solid-state reaction is greatly inhibited due to close packing of the chromophores.[21] In the LB film, the reaction proceeds to some extent, but the efficiency is much lower than that in the liquid phase.[21]

(28) Kunitake, T.; Okahata, Y. *J. Am. Chem. Soc.* **1977**, *99*, 3860.
(29) Adamson, A. A.; Vogler, A.; Kunkely, H.; Wachter, R. *J. Am. Chem. Soc.* **1978**, *100*, 1298.
(30) Griffiths, J. *Chem. Soc. Rev.* **1972**, *1*, 481.

In contrast, by preparing the cis form of film **3** initially by UV illumination at room temperature and then cooling it down to 12 K in a cryostat, we were able to achieve essentially complete photoisomerization from cis to trans (conversion efficiency ca. 100%), even at low temperature (Figure 4b). This is because the initial cis state, which occupies a larger geometric volume than the trans state, requires no additional space for the photoisomerization. Moreover, when the isomerized trans form was then illuminated with UV light at 12 K, the trans-to-cis photoisomerization proceeded to a significant degree, with a conversion efficiency of ca. 60% (process (i) in Figure 4c). The overall trans−cis isomerization cycle was then repeated several times (100% trans to 60% cis) by means of alternating illumination with visible (process (ii) in Figure 4c) and UV light (process (i) in Figure 4c).

Characterization of the Intercalated Film. An elemental analysis of the **3**-Fe$(CN)_6$ film showed that the Fe content was 0.22 wt %. This corresponds to an almost complete anion exchange with the bromide ion of film **3**. Incorporation of $[Fe^{III}(CN)_6]^{3-}$ in film **3** was supported by ^{57}Fe Mössbauer spectroscopy. The Mössbauer spectrum of the **3**-Fe$(CN)_6$ film (not shown) exhibited a doublet with an isomer shift (IS) of -0.01 ± 0.05 mm/s and a quadrupole splitting (QS) of 0.59 ± 0.05 mm/s. Conversely, the spectrum of bulk $K_3Fe^{III}(CN)_6$ shows a doublet with an IS of -0.12 mm/s and a QS of 0.30 mm/s.[31] Structural anisotropy, including chemical environment as well as electrostatic interactions, influences the electronic properties of the interlayer complex. Therefore, the symmetry of the environment surrounding the $[Fe(CN)_6]^{3-}$ ion affects the Mössbauer parameters, depending on the alkylammonium counterions, and the shift in the Mössbauer parameters of the **3**-Fe$(CN)_6$ film compared with those of bulk ($K_3Fe^{III}(CN)_6$) is within the range observed by varying such counterions.[32]

As described in the Experimental Section, the formation of the Fe−CN−Fe framework in film **3** was accomplished by immersing the **3**-Fe$(CN)_6$ film in an aqueous solution of $FeCl_2$.[33] Figure 5a shows a SEM image of the resulting film, designated **3**-Fe$(CN)_6$-Fe. The relative amount of Fe in the film was measured using EDS along the line indicated in Figure 5a. This analysis (Figure 5b) suggests that the intercalated Prussian blue exists inside the vesicles, not outside.

The UV absorption and Mössbauer spectra also suggest the existence of Prussian blue inside the vesicles. The absorption spectrum of the **3**-Fe$(CN)_6$-Fe film revealed a broad peak centered at 726 nm, which is related to the intermetal charge-transfer band from Fe^{II} to Fe^{III}. This absorption maximum, λ_{max}, is red-shifted by ca. 26 nm from that of bulk Prussian blue.[34] This suggests that the Fe(III) ion at the surface of the complex is coordinated by anionic hexacyanoferrate(II) ion to a lesser extent compared to hexacoordinated Fe(III) in the bulk. In addition, it is likely that the surface of the μ-cyanide complex is in contact with the cationic bilayer surface. The existing electrostatic field will therefore lower the Coulombic energy necessary for transferring an electron from hexacyanoferrate(II) ion to the surface Fe(III) species, thus resulting in the red-shifted absorption spectrum.[35] For Prussian blue intercalated into vesicles of films with various **1:2** ratios, such as 10:0 (i.e., with no azobenzene moiety), 10:1 (**3**-Fe$(CN)_6$-Fe), 9:2, and 7:3, the absorption peak was observed at 735, 726, 720, and 719 nm, respectively, showing that the λ_{max} for Prussian blue is very sensitive to the electrostatic interactions between the bilayers and the intercalated Prussian blue. An ^{57}Fe Mössbauer spectrum for **3**-Fe$(CN)_6$-Fe also reflects the electronic interactions between the bilayers and the intercalated Prussian blue. Its Mössbauer spectrum exhibited an Fe^{II} (low-spin) singlet (23.2%, IS $= -0.17 \pm 0.03$ mm/s) and an Fe^{III} (high-spin) doublet (76.8%, IS $= 0.34 \pm 0.03$ mm/s, QS $= 0.66 \pm 0.03$ mm/s). On the other hand, the spectrum of bulk Prussian blue shows a singlet (IS $= -0.24$ mm/s) and a doublet (IS $= 0.32$ mm/s, QS $= 0.57$ mm/s), in which the Fe^{II}/Fe^{III} ratio is close to 3:4.[36] This is consistent with the existence of an electrostatic field, which lowers the Coulombic energy necessary for transferring an electron from hexacyanoferrate(II) ion to the surface Fe(III) species.

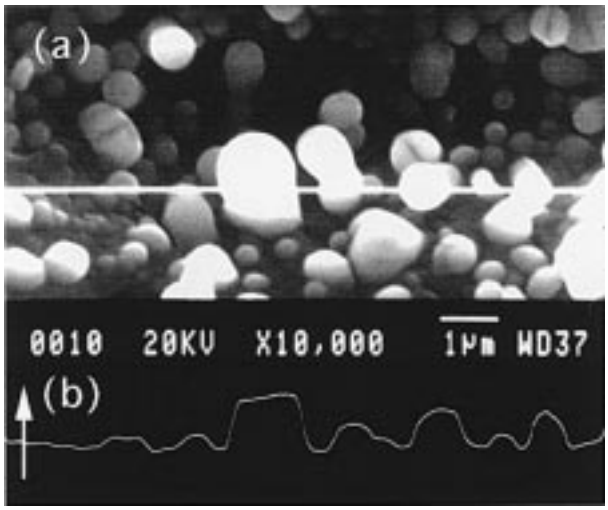

Figure 5. (a) SEM image of **3**-Fe$(CN)_6$-Fe. (b) EDS analysis along the line indicated in part (a), showing the relative intensity for Fe along the line (arrow indicates increasing intensity).

The Change of Magnetic Properties by Photoillumination. In Figure 6 is shown the field-cooled magnetization curve at an external magnetic field of 5 G for the cis form of the **3**-Fe$(CN)_6$-Fe film, which exhibits ferromagnetic properties with a critical temperature (T_c) of 4.2 K. This T_c value is almost identical to that of bulk Prussian blue.[37] We observed the influence of light illumination on the magnetic properties of the film as follows. The cis state of the **3**-Fe$(CN)_6$-Fe film, prepared by UV illumination of the trans film at room temperature, was cooled to 2 K in a SQUID magnetometer. In Figure 7 are shown the magnetization changes for the thus-prepared cis film resulting from alternate illumination with visible light and UV light at 2 K. During the visible light illumination (400−700 nm, power ≈ 1.0 mW/cm^2, 10 min) (step 1), the magnetization value increased from 4.30×10^{-2} to 4.36×10^{-2} emu/g. Even after the illumination wsa stopped, this

(31) Hozony, Y. *Discuss. Faraday Soc.* **1969**, *48*, 148.

(32) Katada, M.; Uchida, Y.; Iwai, K.; Sano, H.; Sakai, H.; Maeda, Y. *Bull. Chem. Soc. Jpn.* **1987**, *60*, 911.

(33) We performed IR measurements to determine the stoichiometry in each step. The **1:2** ratio was determined qualitatively by measuring the ratio of the peaks due to **1** and **2**. However, we could not distinguish between **1** and **2** because of the strong peaks due to PVA. Therefore, to check the **1:2** ratio in each step, we prepared the film without PVA and intercalated $Fe(CN)_6^{3-}$ and Prussian blue into the film on a CaF_2 substrate. **1** and **2** have characteristic peaks at 3423, 2923, and 2853 cm^{-1} and at 3220, 1424, and 1145 cm^{-1}, respectively. The (**1** + **2**) film shows peak intensity ratios 3423 cm^{-1}:2923 cm^{-1}:2853 cm^{-1}:3220 cm^{-1}:1424 cm^{-1}:1145 cm^{-1} = 1:6:3:1:1:1. After intercalation, (**1** + **2**)-Fe$(CN)_6$ and (**1** + **2**)-Fe$(CN)_6$-Fe also had identical peak intensity ratios 3423 cm^{-1}:2923 cm^{-1}:2853 cm^{-1}:3220 cm^{-1}:1424 cm^{-1}:1145 cm^{-1} = 1:6:3:1:1:1. This indicates that the **1:2** stoichiometry is retained during the stepwise synthesis process.

(34) Itaya, K.; Ataka, T.; Toshima, S. *J. Am. Chem. Soc.* **1982**, *104*, 4767.

(35) Robin, M. B. *Inorg. Chem.* **1962**, *1*, 337.

(36) Fluck, E.; Kerler, W.; Neuwirth, W. *Angew. Chem., Int. Ed.* **1963**, 2, 277.

(37) Ito, A.; Suenaga, M.; Ono, K. *J. Chem. Phys.* **1968**, 48, 3597.

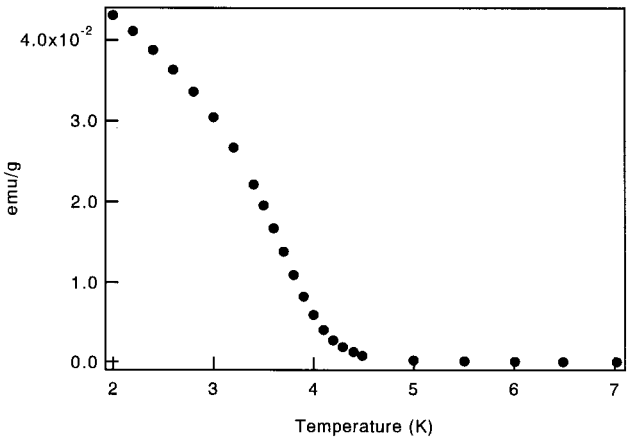

Figure 6. Field-cooled magnetization curve with an external magnetic field of 5 G at 2 K for the cis form of the **3**-Fe$(CN)_6$-Fe film. This film exhibits ferromagnetic properties with a critical temperature of T_c = 4.2 K.

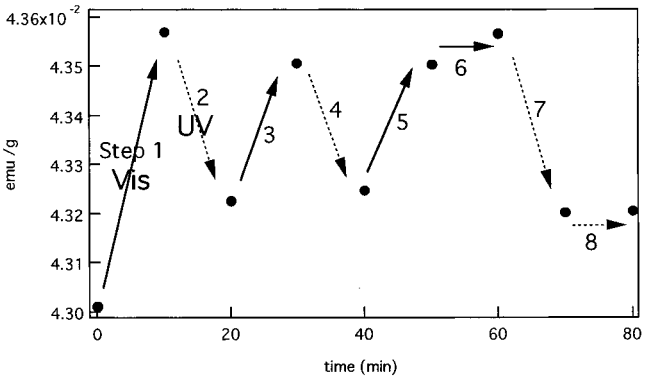

Figure 7. Changes in the magnetization for a **3**-Fe$(CN)_6$-Fe film induced by visible light and UV illumination at 2 K with an external magnetic field of 5 G. The film initially consisted of the cis form, which was prepared by UV illumination of the trans film at room temperature and then cooling the film to 2 K. During each step, the illumination was continued for 10 min. From step 1 to step 5, visible light (solid arrows) and UV light (dashed arrows) were alternated. During steps 5 and 6, the visible illumination was continued (total 20 min), and during steps 7 and 8, the UV illumination was continued (total 20 min). Because all of the magnetization values are subject to small errors due to the photoisomerization state of the film and the SQUID measurement, the values obtained after steps 1, 3, 5, and 6 are estimated to be approximately equal, while the values obtained after steps 2, 4, 7, and 8 are also estimated to be approximately equal.

increased magnetization was maintained for at least 2 h. Then we illuminated the sample with UV light (360 nm, power $\approx$ 1.0 mW/cm^2) for a further 10 min (step 2). The magnetization value decreased ca. 60% (to ca. 4.32×10^{-2} emu/g). This value in the changes of the magnetization is consistent with that of the UV−vis spectral change shown in Figure 4b,c. After step 2, the visible light-induced increase and UV light-induced decrease of the magnetization were repeated several times, from step 2 through step 5. Extended illumination with visible light (step 6) or UV light (step 8) (greater than 10 min) did not produce further changes in the magnetization; i.e., the photo-induced magnetization changes saturated after a 10-min illumination. These magnetization changes are consistent with the UV−visible absorption spectral changes and can be explained in the same fashion.

When the **3**-Fe$(CN)_6$-Fe film was prepared without washing during the stepwise synthesis process, bulk Prussian blue was formed *outside* the vesicles, and photoillumination produced

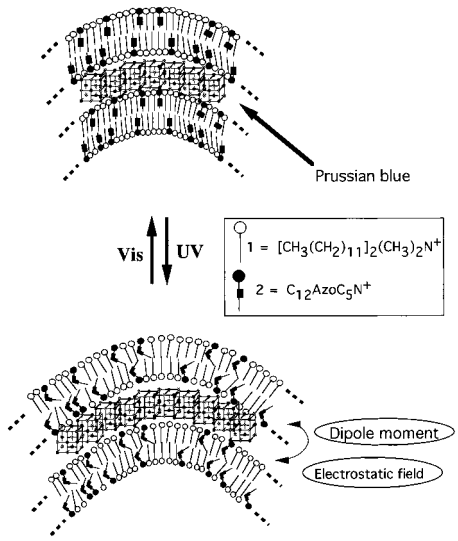

Figure 8. Schematic illustration of the geometrically confined structural transformations induced by photoillumination. Photoisomerization of **2**, assumed to be randomly dispersed within the **1** bilayer, affects the vesicle structure, and there is a concomitant pressure change acting upon the intercalated Prussian blue. As a result, the dipole moment and electrostatic field are affected.

only very small changes (~0.2%) in the total magnetization. This result suggests that the photoillumination affects only the Prussian blue intercalated *inside* the vesicles. Furthermore, there was no photoillumination effect in either the **1**-Fe$(CN)_6$-Fe film, i.e., without the azobenzene moiety, or in bulk Prussian blue, i.e., without the photoisomerizing bilayer membrane. On the basis of the above results, we have concluded that the magnetization control by light illumination is due to the photoisomerization of the bilayer membrane. Turbidity (optical absorbance of the film at 662 nm) measurements also indicated that the photoisomerization of the azo moiety in film **3** induced the changes in the vesicle structure.[38]

Figure 8 shows a schematic illustration of the structural change. It is proposed that photoisomerization of the film is accompanied by a geometrically confined structural change, as reflected by changes in dipole moment and electrostatic field. Therefore, the magnetization values could be switched reversibly with successive UV and visible light illumination.

Summary

We have designed a new photofunctional composite material comprising Prussian blue intercalated into photoresponsive vesicles whose magnetic properties can be controlled by photoillumination. Our results suggest that this phenomenon is

(38) To understand how the cis−trans structural change affects the magnetization change, we investigated the relationship between the molecular cis−trans transformation for azobenzene and the *submicrometer*-scale structural change occurring in the vesicles. The structural changes involving the vesicles were monitored by measuring the optical absorbance (turbidity) of the film at 662 nm (A_{662}). Because the azobenzene moiety does not absorb light at 662 nm, the infinitesimal absorbance changes at this wavelength reflect the *submicrometer*-scale changes in the vesicle structure. The A_{662} value of film **3** (=**1**(vesicle) + **2**(Azo) + PVA) decreased from 0.0701 (trans) to 0.0698 (cis) with UV illumination, and the reverse process was observed upon visible light illumination. Conversely, for the (**2**(Azo) + PVA) film, which did not form vesicles, the A_{662} values did not change, even though the photoisomerization proceeded. Moreover, for the (**1**(vesicle) + PVA) film, which does not contain the azobenzene moiety, the A_{662} values did not change as a result UV illumination, even though vesicles were present.

due to changes in the vesicle structure induced by the photoisomerization of azobenzene. We believe that this small structural change affects the electrostatic interactions between the Prussian blue and the vesicle bilayer. The present work offers new perspectives into photofunctional materials derived from the combination of a functional bilayer assembly and a molecule-based magnetic material. Further attempts to intercalate materials layer by layer into other functional organic molecules at the *nanometer* scale will open many possibilities in the development of new superior functional materials.

Acknowledgment. We thank Dr. Y. Kobayashi and Dr. F. Ambe of The Institute of Physical and Chemical Research (RIKEN) for making the Mössbauer facility available to us and Prof. T. Watanabe and Mr. N. Fukumuro, Tokyo Metropolitan University, and Dr. P. Sawunyama and Prof. D. A. Tryk for useful discussions. This work was supported by a Grant-in-Aid for Scientific Research on Priority Areas, Electrochemistry of Ordered Interfaces, from the Ministry of Education, Science, Sports and Culture of Japan.

JA982450L